

A. DI GERLANDO, R. PERINI, I. VISTOLI

DESIGN AND EXPERIMENTAL INVESTIGATION OF  
THE VOLTAGE DISTORTION OF SALIENT-POLE  
SYNCHRONOUS GENERATORS

ICHQP VII  
7th International Conference on  
Harmonics and Quality of Power

Las Vegas, NV (USA)  
October 16-18, 1996

# Proceedings of the



## 7<sup>th</sup> INTERNATIONAL CONFERENCE ON HARMONICS AND QUALITY OF POWER

October 16 - 18, 1996  
Las Vegas, Nevada, USA

Co-Sponsored by



# DESIGN AND EXPERIMENTAL INVESTIGATION OF THE VOLTAGE DISTORTION OF SALIENT-POLE SYNCHRONOUS GENERATORS

A. Di Gerlando, *Member, IEEE*

R. Perini

I. Vistoli

Dipartimento di Elettrotecnica, Politecnico di Milano  
Piazza Leonardo da Vinci, 32 - 20133 Milano

**Abstract** - A method for the evaluation of the harmonic distortion of the no-load voltage of salient-pole synchronous generators is described and applied, based on the solution of non-linear, time-varying magnetic networks. The links between the time waveform of the flux in the teeth and the waveforms of the flux linkage and of the phase winding e.m.f. are shown; the dependence of the harmonic distortion on the design parameters is analysed. An example of application using a standard alternator is considered, comparing the results of the calculations and of the experimental tests.

## INTRODUCTION

The Standards fix defined constraints about the no-load voltage waveform of salient-pole alternators, by means of the total harmonic distortion (THD) and of the telephonic harmonic factor (THF): the constructional parameters affecting this distortion are numerous and it is important to evaluate their effects during the design, in such a way to satisfy as better as possible the waveform requirements.

To this aim, in some previous papers [1], [2], [3] a method for the evaluation of the no-load voltage harmonic distortion has been developed, that takes into account the presence of the teeth, the winding characteristics, the saturation in all the ferromagnetic branches and the skewing between rotor and stator: this method leads to calculate the waveform by a subsequent solving of suited equivalent magnetic networks of the machine, repeated for various stator-rotor positions. The  $N^\circ$  of these positions must be adequate to obtain the harmonic e.m.f. with the higher order of interest [1].

After the description of the method characteristics, the link between the tooth flux waveform and the phase flux linkage waveform is analytically investigated, showing the transformation of this link in a similar connection between the corresponding harmonics: this allows to separate the distortion effects due to the geometrical features of the magnetic circuit (air-gap, shape of the pole shoes, slot skewing,...) from the distortion effects connected to the characteristics of the adopted winding (particularly the coil pitch).

Subsequently, a standard synchronous generator is considered: different quantities concerning this machine are obtained, by means of calculations and experimental tests:

- waveform and harmonics of the flux in the teeth;
- harmonics of the line-to-neutral and of the line-to-line e.m.f.;
- dependence of the harmonic distortion on the field current.

The discrepancies between calculations and tests are analysed, and the effects of the machine constructional dissymmetries, due to the manufacture tolerances, are discussed; the link between the distortion level and the variation of some dimensional and functional parameters is investigated.

## FEATURES OF THE METHOD FOR THE EVALUATION OF THE NO-LOAD VOLTAGE WAVEFORM

The method for the determination of the e.m.f. waveform of a synchronous generator is based on the use of an equivalent magnetic network of the machine; the method has the following features:

- it can be used with any kind of winding and magnetic structures;
- the set of equations is obtained easily and automatically.

In the more general case (in which we want to consider possible constructional dissymmetries), this network corresponds to the overall machine and it contains the following circuit elements:

- constant reluctances (leakage reluctances between adjacent poles: their number equals the number of poles "p");
- position-dependent linear reluctances at the air-gap (between each tooth and the pole faced to it, in the following called tooth permeances at the air-gap: their  $N^\circ$  equals the  $N^\circ$  of slots "s");
- saturable reluctances: teeth reluctances (whose  $N^\circ$  is s), reluctances of the stator yoke segments among adjacent teeth (whose  $N^\circ$  is s), pole body reluctances (whose  $N^\circ$  is p), reluctances of the rotor yoke segments between adjacent poles (whose  $N^\circ$  is p);
- field m.m.f.s (series connected with each pole body reluctance, with alternated signs).

As regards the tooth reluctances at the air-gap, for each rotor-stator position, the singling out of the pole magnetically faced to each tooth depends on the position of the axis of every tooth as regards the rotor polar arcs; two cases occur:

- the tooth has the tooth pitch totally belonging to the pole pitch of one rotor pole: in this case, the air-gap permeance of this tooth is evaluated on the basis of just one flux tube;
- the tooth has the tooth pitch crossed by an interpolar axis: in this case it is represented by a permeance connected to the nearest pole, evaluated as a difference between the permeances of the two flux tubes between the tooth itself and the two adjacent poles [1].

Among all the quantities of the equivalent network, the tooth reluctance at the air-gap is the most difficult parameter to be evaluated, because it depends on the map of the magnetic field at the air-gap.

In the present circuit-based method, this reluctance is evaluated by means of an approximate representation of the field lines and evaluating the following, well known, integral:

$$\lambda_g = \mu_0 \cdot \int_{\tau_t} \frac{d\tau_t}{b_g}, \quad \text{where} \quad (1)$$

- $\lambda_g$  is the tooth permeance at the air-gap, per unit length of the machine in the axial direction;
- $\tau_t$  is the air-gap tooth pitch, i.e. the cross-section at the air-gap corresponding to a tooth pitch, again per unit length;
- $b_g$  is the length of the generic field line at the air gap, that develops within the tooth pitch of the considered tooth.

The procedure (verified also by means of some numerical simulations using the Finite Element Method) is based on the approximate evaluation of the length  $b_g$  of the field lines by using polygonal lines [2]; each line having length  $b_g$  is subdivided as follows:

- field line among the pole shoe and the internal stator circumference, with length  $b_{g1}$ ;
- field line among the stator internal circumference and the tooth side, with length  $b_{g2}$  (of course,  $b_{g2}$  is zero in the case the air-gap field line reaches directly the tooth head).

The usefulness of this subdivision comes from the assumption that the length  $b_{g1}$  does not depend on the presence of the teeth: on the other hand, the field concentration effect at the teeth heads is important only under the pole shoe, where it is possible to take it into account by using a correction coefficient based on the Carter's factor.

As regards the skewing between stator and rotor, if this skewing is zero, the tooth permeance at the air-gap equals:

$$\Lambda_g = \lambda_g \cdot \ell, \quad (2)$$

where  $\ell$  is the axial length of the machine: in this case the magnetic network is extended to this total length. Vice versa, in case of skewing, it is necessary to axially subdivide the machine in several segments, each represented by a different magnetic network; the solution of these networks for each position gives the flux contribution of the various segments: the sum of these partial fluxes, performed tooth by tooth, gives the global fluxes of the teeth.

For every rotor-stator position, the evaluation of the fluxes of each magnetic network is obtained by means of the mesh analysis method. Supposing that we travel along the stator periphery in the clock-wise sense and that each tooth has the same order  $N^\circ$  of the preceding slot, the numbering sequence of these magnetic meshes is the following one: at first the "s" slot meshes; thus the "p" inter-polar meshes; finally the rotor yoke mesh; therefore, there are

$$N_m = s + p + 1 \quad (3)$$

magnetic meshes, with the same  $N^\circ$  of unknown fluxes ( $\varphi_{mk}(t)$ ).

The set of equations is the following one:

$$[\theta] \cdot [\varphi_m] = [M], \quad (4)$$

$$\text{or, in other terms: } \begin{bmatrix} [\theta_s] & [\theta_{sr}] \\ [\theta_{sr}]^t & [\theta_r] \end{bmatrix} \cdot \begin{bmatrix} [\varphi_{ms}] \\ [\varphi_{mr}] \end{bmatrix} = \begin{bmatrix} [0] \\ [M_r] \end{bmatrix} \quad (5)$$

The matrix  $[\theta]$  is symmetrical, with dominant diagonal and it includes the following sub-matrices:

- $[\theta_s]$ , matrix of the self and mutual reluctances of the stator slots; it is squared, of order  $s$ ; each mesh corresponds to one slot and for each row of  $[\theta_s]$  there are only 3 terms different from zero, considering that each slot is adjacent to other two slots only;
- $[\theta_r]$ , matrix of the self and mutual rotor reluctances, squared too, with order  $p + 1$ ;
- $[\theta_{sr}]$ , matrix of the mutual reluctances between stator and rotor; it has  $s$  rows and  $p + 1$  columns; the only non-zero elements are the leakage reluctances between poles.

The vectors  $[\varphi_{ms}]$  (with order  $s$ ) and  $[\varphi_{mr}]$  (with order  $p + 1$ ) contain the stator and rotor mesh fluxes, while  $[M_r]$  includes the mesh m.m.f.s of the rotor.

For solving the system (4), an iterative method is used, based on the gradual upgrading of the permeabilities of the saturable branches, [1]; the knowledge of the stator mesh fluxes leads to evaluate (by difference) the teeth fluxes:  $\varphi_k(t)$ , with  $k = 1, 2, \dots, s$ .

In case of a machine that is symmetrical from the constructional point of view, it is possible and convenient to limit the magnetic network to the minimum necessary peripheral portion, equal to that of an electromagnetic cycle [1].

#### **TOOTH FLUXES, PHASE FLUX LINKAGE AND E.M.F. HARMONICS: LINKS IN THE TIME DOMAIN AND IN THE FREQUENCY DOMAIN**

Called  $\gamma(t)$  the electrical angle between prefixed rotor and stator positions ( $\gamma$  positive in the counter clock-wise direction), let us suppose that, by solving the system (4) for each  $\gamma$  value, we know the teeth fluxes  $\varphi_k(\gamma(t)) = \varphi_k(t)$ , with  $k=1, 2, \dots, s$ , i.e. the vector  $[\varphi(t)]$ . The waveform of the flux linkage  $\psi_{cj}(t)$  of the  $j^{\text{th}}$  coil of the considered phase winding can be expressed as follows:

$$\psi_{cj}(t) = N \cdot \sum_{k=1}^s a_{jk} \cdot \varphi_k(t) = N \cdot [a_j]^t \cdot [\varphi(t)] \quad (6)$$

where  $a_{jk}$  equals +1 or 0 if the  $j^{\text{th}}$  coil (with  $N$  turns) includes or not the  $k^{\text{th}}$  tooth respectively.

The vector of the flux linkages of the  $m$  series-connected coils of the phase windings can be expressed as follows:

$$[\psi_c(t)] = N \cdot [A] \cdot [\varphi(t)] \quad (7)$$

in eq.(7) the  $j^{\text{th}}$  row of  $[A]$  is the vector  $[a_j]^t$  of eq.(6);  $[A]$  can be called teeth-coil linking matrix: apart from the sign, it describes the linkage of the teeth with each of the  $m$  coils of every phase winding path. Finally, the total flux linkage of each path is given by:

$$\psi(t) = \sum_{j=1}^m b_j \cdot \psi_j = [B]^t \cdot [\psi_c(t)] \quad (8)$$

$[B]$  is the vector of the linkage signs:  $b_j$  equals +1 if the coil versor coincides with that assumed positive for the teeth fluxes, while it equals -1 if the two versors are opposite (i.e. in case of inverted terminal coil connection).

On the basis of eq.s (6)-(8), the flux linkage  $\psi(t)$  and the vector of the teeth fluxes  $[\varphi(t)]$  are linked as follows:

$$\psi(t) = N \cdot [c] \cdot [\varphi(t)] = [C] \cdot [\varphi(t)] \quad (9)$$

$$\text{where } [c] = [B]^t \cdot [A] \quad (10)$$

$[c]$  and  $[C]$  are both row vectors;  $[c]$ , defined linkage vector, takes into account the distribution of the phase winding coils in the slots, while  $[C]$  is the global linkage vector and it includes  $N$ , number of turns of each coil. The element  $c_k$  with position  $k$  in the vector  $[c]$  gives the number of linkages (with the suited sign) of the  $k^{\text{th}}$  tooth with the considered phase winding:  $c_k$  is called linkage coefficient.

The knowledge of  $\psi(t)$  allows the direct evaluation of the harmonics of the phase induced e.m.f.  $e(t)$  [1]:

$$e(t) = -\frac{d\psi}{dt} = -\frac{d\psi}{d\gamma} \cdot \frac{d\gamma}{dt} = -\frac{d\psi}{d\gamma} \cdot \omega \quad (11)$$

In fact, by inserting eq.(11) in the Fourier integrals, we have:

$$\begin{aligned} \hat{E}_{ch} &= \frac{2}{T} \cdot \int_0^T e(t) \cdot \cos(h \cdot \omega \cdot t) \cdot dt = -\frac{\omega}{\pi} \cdot \int_0^{2\pi} \frac{d\psi}{d\gamma} \cdot \cos(h \cdot \gamma) \cdot d\gamma \\ \hat{E}_{sh} &= \frac{2}{T} \cdot \int_0^T e(t) \cdot \sin(h \cdot \omega \cdot t) \cdot dt = -\frac{\omega}{\pi} \cdot \int_0^{2\pi} \frac{d\psi}{d\gamma} \cdot \sin(h \cdot \gamma) \cdot d\gamma \end{aligned} \quad (12)$$

by integrating "per parts" the eq.s (12) one obtains:

$$\begin{aligned} \hat{E}_{ch} &= -h \cdot \frac{\omega}{\pi} \cdot \int_0^{2\pi} \psi(\gamma) \cdot \sin(h \cdot \gamma) \cdot d\gamma \\ \hat{E}_{sh} &= +h \cdot \frac{\omega}{\pi} \cdot \int_0^{2\pi} \psi(\gamma) \cdot \cos(h \cdot \gamma) \cdot d\gamma \end{aligned} \quad (13)$$

Finally, the waveform of the  $e(t)$  can be expressed as follows:

$$e(t) = \sum_{h=1}^{h_{\max}} (\hat{E}_{ch} \cdot \cos(h \cdot \omega \cdot t) + \hat{E}_{sh} \cdot \sin(h \cdot \omega \cdot t)) \quad (14)$$

The eq.s (9)-(14) apply in the general situation of a machine that is non perfectly symmetrical from the constructional point of view: in this non-symmetrical situation, the teeth fluxes  $\varphi_k(t)$  of the vector  $[\varphi(t)]$  have different waveforms.

Vice versa, if we consider a perfectly symmetrical machine (typical situation of the design), all the teeth flux waveforms are similar, even if time phase-shifted, and the previous relations can be transformed, leading to corresponding links between harmonic phasors in the frequency domain: this transformation allows to show different, interesting properties, useful for the design.

In any case, it must be observed that the existence of just one shape of tooth flux waveform does not allow to reduce the solution of (4) to that of an equivalent network including just one tooth: in fact, because of the presence of saturable ferromagnetic branches, the calculation of the teeth fluxes requires the simultaneous evaluation of all the magnetic network fluxes, being active all the m.m.f.s.

Called  $\alpha$  the electrical angle between adjacent slots:

$$\alpha = \pi \cdot p/s \quad (15)$$

if  $\varphi_1(t)$  represents the waveform of the tooth  $N^\circ 1$ , in case of symmetrical machine the waveform of the flux in the  $k^{\text{th}}$  tooth equals that of the tooth  $N^\circ 1$ , except for a time phase displacement, proportional to the number  $(k - 1)$  of the interposed slots:

$$\varphi_k(t) = \varphi_1(t + (k-1) \cdot \alpha / \omega) \quad (16)$$

Considering that  $\varphi_k(t)$  is a periodic function (with period  $T=2\pi/\omega$ ), it can be developed in Fourier series, in the following manner:

$$\varphi_k(t) = \sum_{h=1}^{\infty} \Phi_h \cdot \cos[h \cdot \omega \cdot t + \beta_h + h \cdot (k-1) \cdot \alpha] \quad (17)$$

where  $\Phi_h$  is the peak value of the  $h^{\text{th}}$  harmonic of the tooth flux, while  $\beta_h$  is the corresponding phase for the tooth N° 1.

On the basis of (17), by means of the operator  $\text{Re}(\cdot)$  and of eq.s (9) and (10), the phase flux linkage  $\psi(t)$  can be expressed as follows:

$$\psi(t) = N \cdot \sum_{k=1}^s c_k \cdot \sum_{h=1}^{\infty} \text{Re} \left\{ \Phi_h \cdot e^{[j(h \cdot \omega \cdot t + \beta_h + h \cdot (k-1) \cdot \alpha)]} \right\} \quad (18)$$

On the other hand, the order of the two operators  $\Sigma(\cdot)$  and  $\text{Re}(\cdot)$  can be inverted, as like as we can do for the summations, so that:

$$\psi(t) = N \cdot \text{Re} \left[ \sum_{h=1}^{\infty} \bar{\sigma}_h \cdot \bar{\Phi}_h \cdot e^{(j \cdot h \cdot \omega \cdot t)} \right] \quad (19)$$

$$\text{where} \quad \bar{\Phi}_h = \Phi_h \cdot e^{(j \cdot \beta_h)} \quad (20)$$

$$\text{and} \quad \bar{\sigma}_h = \sum_{k=1}^s c_k \cdot e^{[j \cdot h \cdot (k-1) \cdot \alpha]} \quad (21)$$

$\bar{\sigma}_h$  represents a sum of phasors, whose amplitudes are the linkage coefficients ( $c_k$ ) between the teeth and the winding and whose phases depend on the angle between adjacent slots ( $\alpha$ ) and on the considered harmonic order ( $h$ ); thus,  $\bar{\sigma}_h$  can be called "tooth factor", corresponding to the  $h^{\text{th}}$  time harmonic.

In order to better understand the meaning of the tooth factor, it is worth to notice that also the flux linkage  $\psi(t)$  of each path of the phase winding is a periodic function of period  $T$ , thus it can be expressed by means of a Fourier series as follows:

$$\psi(t) = \text{Re} \left[ \sum_{h=1}^{\infty} \Psi_h \cdot e^{[j(h \cdot \omega \cdot t + \xi_h)]} \right] = \text{Re} \left[ \sum_{h=1}^{\infty} \bar{\Psi}_h \cdot e^{[j(h \cdot \omega \cdot t)]} \right] \quad (22)$$

By comparing eq.s (19) and (22), for the generic  $h^{\text{th}}$  harmonic we can write:

$$\bar{\Psi}_h = N \cdot \bar{\sigma}_h \cdot \bar{\Phi}_h \quad (23)$$

On the basis of (11) and (22), the following expression of the peak value of the phasor harmonic phase winding e.m.f. can be written:

$$\bar{E}_h = -j \cdot \omega \cdot h \cdot \bar{\Psi}_h = -j \cdot \omega \cdot N \cdot h \cdot \bar{\sigma}_h \cdot \bar{\Phi}_h \quad (24)$$

Eq.s (23) and (24) show that the tooth factor  $\bar{\sigma}_h$  has a meaning very similar to that of the winding factor  $k_{wh}$  of the classical theory: in fact,  $\bar{\sigma}_h$  performs the summation of the phasors of the teeth harmonic fluxes, taking into account the following quantities:

- number of linkages of each tooth (i.e. the number of coils  $c_k$  of the phase winding that link each tooth  $k$ );
- electrical angle  $h \cdot (k-1) \cdot \alpha$  of the  $h^{\text{th}}$  harmonic flux of the  $k^{\text{th}}$  tooth, referred to the position of the tooth N° 1, corresponding to the considered linkage.

In any case, the quantitative link between the coefficients  $\sigma_h$  and  $k_{wh}$  is not easy to be developed in analytical terms, because these factors are applied to different quantities:  $\sigma_h$  refers to the sum of the tooth harmonic fluxes, while  $k_{wh}$  refers to the sum of the fluxes of each "harmonic magnetic pole"; thus,  $k_{wh}$  refers to the integral at the air-gap of each flux density half-wave (with sinusoidal distribution, extended to the pole pitch of the  $h^{\text{th}}$  spatial harmonic field).

Eq.(24) points out also the different elements that affect the e.m.f. harmonic spectrum, involving both the harmonics of the tooth fluxes and the tooth factors:

- the harmonics of the tooth flux depend on the geometrical characteristics of the magnetic core (air-gap width, shape of the pole shoe, width of the slot opening, rotor-stator skewing) and on its operating conditions (saturation level, due to the value of the field

m.m.f. and to the cross-sections of the different ferromagnetic branches);

- the tooth factor takes into account the features of the winding: in fact, it is a factor (to be applied to the tooth flux harmonics) that depends on the kind of connections between active conductors, on the coil pitch and on the number of slot/(pole-phase).

The structure of eq.(24) allows also to express in a synthetic way the dependence of the THD on the above-mentioned constructional and operating characteristics; in fact, by inserting eq.(24) in the definition of the THD of the phase e.m.f. ( $\text{THD}_{ph}$ ) one obtains:

$$\text{THD}_{ph} = \sqrt{\sum_{h=2}^{\infty} h^2 \cdot \left( \frac{\sigma_h}{\sigma_1} \right)^2 \cdot \left( \frac{\Phi_h}{\Phi_1} \right)^2} \quad (25)$$

The analysis of eq.(25) suggests that:

- the value of  $\text{THD}_{ph}$  is not affected by the absolute values of the tooth factor coefficients and of the harmonic tooth fluxes, but by their p.u. values, referred to the corresponding fundamental values;
- a low value of the ratio  $\sigma_h/\sigma_1$  (that can be obtained by modifying the winding characteristics) can help in reducing the effect of some harmonic tooth fluxes, except for the so-called "tooth harmonics", for which  $\sigma_h/\sigma_1$  equals unity (see in the following);
- the limitation of the  $\text{THD}_{ph}$  requires mainly the reduction of the harmonics of the tooth flux (that can be obtained by optimising the extension and the shape of the pole shoe and by realising the stator-rotor skewing).

If we consider the line-to-line voltages instead of the line-to-neutral ones, by applying the suited phase displacements one obtains the following expression of the RMS value of the no-load line-to-line voltage ( $E_{Lh}$ ), as a function of the harmonic tooth flux:

$$E_{Lh} = \sqrt{1 - \cos(h \cdot 2 \cdot \pi / 3)} \cdot \omega \cdot N \cdot h \cdot \sigma_h \cdot \Phi_h \quad (26)$$

As well known, eq.(26) points out that in the line-to-line voltage all the 3<sup>rd</sup> harmonics and multiples are zero, while the remaining harmonics equal  $\sqrt{3}$  times the corresponding phase harmonics.

As a consequence, the THD of the line-to-line voltage ( $\text{THD}_L$ ) is:

$$\text{THD}_L = \sqrt{\frac{2}{3} \cdot \sum_{h=2}^{\infty} \left[ 1 - \cos \left( h \cdot \frac{2 \cdot \pi}{3} \right) \right] \cdot h^2 \cdot \left( \frac{\sigma_h}{\sigma_1} \right)^2 \cdot \left( \frac{\Phi_h}{\Phi_1} \right)^2} \quad (27)$$

Eq.(27) suggests the same remarks done for eq.(25), also considering that the expression of  $\text{THD}_{ph}$  reduces to that of  $\text{THD}_L$  in the case that all the 3<sup>rd</sup> and multiple harmonics are cancelled in the summation of  $\text{THD}_{ph}$ ; of course, for the two THDs we can write:

$$\text{THD}_{ph} \geq \text{THD}_L \quad (28)$$

in eq.(28) the equal sign occurs when the line-to-neutral e.m.f. itself does not include the 3<sup>rd</sup> and multiple harmonics.

It is worth to repeat that eq.s(24)-(27) apply only to a perfectly symmetrical machine from the constructional point of view.

In order to show the properties of  $\sigma_h$ , the machine of Table I is considered, in the following used also for the experimental tests.

Table I - Main nominal data of the synchronous generator used for the calculations and the tests (the damping cage is absent;  $I_{e0}$  is the field current necessary to give the rated voltage at no-load).

$A_n$ [kVA]; $f_n$ [Hz]; poles	13; 50; 4
Nom. V: $V_n$ [VRMS]; nom. field current $I_{e0}$ [A <sub>dc</sub> ]	380; 2
diameter: $D$ [mm]; length: $\ell$ [mm]	160; 180
air-gap at the centre of the pole: $\delta$ [mm]	0.6
pole shoe width $b_e$ [mm]; $\delta_{\max}$ [mm]	74; 1.12
stator-rotor skewing (in N° of slots)	1.5
stator: N° of layers/slot; N° of turns/coil: N	2; 24
stator: N° of slots: $s$ ; coil pitch: $y_c$	30; 5
stator: N° of paths in parallel	2
rotor: N° of field turns/pole	300

Considering that the electromagnetic cycle is extended to 2 poles, it is enough to consider just 15 slots of the  $s = 30$  total slots of the machine; within this periphery portion there are 5 coils belonging to one of the two paths of the phase winding. It follows that the vector [B] of the linkage signs (see eq.(8)) equals:

$$[B]^t = [1 \ 1 \ -1 \ -1 \ -1] ;$$

the negative sign of the last three coefficients means that the corresponding coils are counter-connected as regards the others, because they are under the influence of an opposite sign magnetic pole.

The teeth-coil linking matrix [A] (see eq.(7)) depends on the coil pitch  $y_c$ ; considering that we want to show what happens with different values of  $y_c$ , it is convenient to mark this matrix as follows:  $[A]_{(y_c)}$ ; for the cases  $y_c = 5$  and  $y_c = 6$  we have, respectively:

$$[A]_{(5)} = \begin{bmatrix} 1 & 1 & 1 & 1 & 1 & 0 & 0 & 0 & 0 & 0 & 0 & 0 & 0 & 0 & 0 \\ 0 & 1 & 1 & 1 & 1 & 1 & 0 & 0 & 0 & 0 & 0 & 0 & 0 & 0 & 0 \\ 0 & 0 & 0 & 0 & 0 & 0 & 0 & 1 & 1 & 1 & 1 & 1 & 0 & 0 & 0 \\ 0 & 0 & 0 & 0 & 0 & 0 & 0 & 0 & 1 & 1 & 1 & 1 & 1 & 0 & 0 \\ 0 & 0 & 0 & 0 & 0 & 0 & 0 & 0 & 0 & 1 & 1 & 1 & 1 & 1 & 0 \end{bmatrix},$$

$$[A]_{(6)} = \begin{bmatrix} 1 & 1 & 1 & 1 & 1 & 1 & 0 & 0 & 0 & 0 & 0 & 0 & 0 & 0 & 0 \\ 0 & 1 & 1 & 1 & 1 & 1 & 1 & 0 & 0 & 0 & 0 & 0 & 0 & 0 & 0 \\ 0 & 0 & 0 & 0 & 0 & 0 & 0 & 1 & 1 & 1 & 1 & 1 & 1 & 0 & 0 \\ 0 & 0 & 0 & 0 & 0 & 0 & 0 & 0 & 1 & 1 & 1 & 1 & 1 & 1 & 0 \\ 0 & 0 & 0 & 0 & 0 & 0 & 0 & 0 & 0 & 1 & 1 & 1 & 1 & 1 & 1 \end{bmatrix}.$$

As it can be observed, the matrixes [A], rather sparse, are different just for the number of unit elements present within each row.

By performing the products indicated in eq.(10), the row vectors  $[c] = [B]^t \cdot [A]$  of the linkage coefficients can be obtained:

$$[c]_{(5)} = [1 \ 2 \ 2 \ 2 \ 2 \ 1 \ 0 \ -1 \ -2 \ -3 \ -3 \ -3 \ -3 \ -2 \ 0]$$

$$[c]_{(6)} = [1 \ 2 \ 2 \ 2 \ 2 \ 2 \ 1 \ -1 \ -2 \ -3 \ -3 \ -3 \ -3 \ -3 \ -2 \ -1].$$

Apart from the signs, the presence in the vector  $[c]_{(6)}$  of some coefficients that are higher compared with those of  $[c]_{(5)}$  shows that the winding with the coil pitch  $y_c = 6$  has a higher number of teeth linked with the coils.

The application of eq.(21) to the 2 vectors  $[c]$  now evaluated leads to the diagrams of fig.1, that show the value of the amplitudes of the toothling coefficients  $\sigma_h$  as a function of the considered harmonic.

The following remarks can be made:

- the values of  $\sigma_h$  as a function of  $h$  appear to be periodic, with period 15: thus, it is sufficient to evaluate the values of  $\sigma_h$  up to the 15<sup>th</sup> harmonic, because the subsequent values repeat themselves regularly; this property is due to the fact that, being  $\alpha = 2\pi/15$ , with  $h = 15$  the product  $h \cdot \alpha$  satisfies the condition:  $h \cdot \alpha = 2\pi$ ; for eq.(18), it follows that all the phasors tooth fluxes have the same phase; thus,  $h$  values higher than 15 produce the same displacements that occur with harmonic orders  $(h - 15)$ : thus, the repetition of the portion of the spectrum for  $1 < h < 15$  occurs;
- there are some harmonic orders for which  $\sigma_h$  has the same value of  $\sigma_1$ , corresponding to the fundamental field: this happens exactly in the same circumstances for which the equivalence between the winding factors occurs, i.e. for the harmonic orders of the so-called "tooth harmonic" fields; indicated with  $q = s/(3 \cdot p)$  the number of slots per pole and per phase, the harmonic orders of these tooth harmonic fields equal:

$$h_t = 1 + K \cdot 6 \cdot q, \quad \text{con } K = \pm 1, \pm 2, \dots,$$

i.e., in this case:  $|h_t| = |1 + K \cdot 15| = 14, 16, 29, 31, \dots$ ;

- the value of  $\sigma_1$  in the case  $y_c=6$  ( $\sigma_1 = 21.88$ ) is higher than that of the case  $y_c = 5$  ( $\sigma_1 = 19.92$ ); moreover, the ratio between these values of  $\sigma_1$  ( $21.88/19.92$ ) equals the ratio between the corresponding fundamental harmonic winding factors ( $0.9099/0.8285$ );

- in the case  $y_c = 5$  (that of the actually tested machine) the toothling factors of the following harmonics multiple of 3 are zero: 3, 6, 9, 12, 18, 21, 24, 27, 33, ...; thus, again in the hypothesis of machine symmetrical from the constructional point of view, even if these harmonics are present in the waveform of the tooth flux, they are cancelled in the phase flux linkage, and therefore also in the corresponding harmonics of the phase e.m.f.;
- again in the case  $y_c = 5$  it can be observed that the toothling factors for  $h = 15, 30, 45, \dots$  are different from zero, differently from what happens for the corresponding winding factors, that are zero: in fact, for the above-mentioned values of  $h$  all the tooth flux harmonics have the same phase: it follows that  $\sigma_h$  equals the algebraic sum of the linkage coefficients  $c_k$  (in this case  $|\sigma_h| = 5$ );
- in case of  $y_c = 6$  the toothling factors of the following harmonics multiple of 5 are zero: 5, 10, 20, 25, 35, ...; vice versa, the harmonic fluxes with order 3 and multiples are different from zero; comments similar to the previous ones can be applied, in particular for  $h = 15, 30, 45, \dots$ ;
- as regards the tooth flux harmonics, it must be observed that, again in case of symmetrical machine, in the no-load operation the even harmonics have always exactly zero values, because their presence could be caused only by a constructional dissymmetry between adjacent rotor poles.

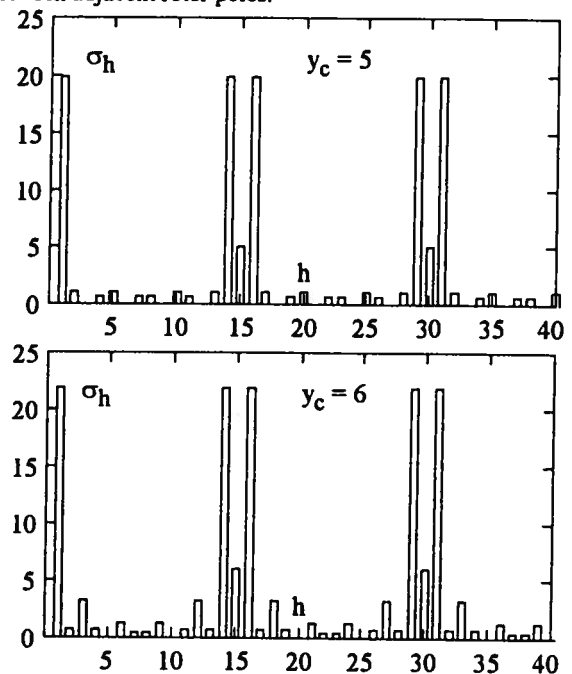


Fig.1 - Histograms of the amplitudes of the toothling factor  $\sigma_h$  as a function of the harmonic order  $h$ , for the synchronous machine with the data of Table I;  $y_c=5$  (above) and  $y_c=6$  (below); the values of  $\sigma_h$  refer to one electromagnetic cycle (2 poles).

Again in the hypothesis of a symmetrical machine, in the case of  $y_c = 5$  the disagreement between winding and toothling factors for  $h = 15, 30, 45, \dots$  can be explained by considering the physical meaning of the phase accordance of these particular tooth harmonic fluxes:

- the winding factors consider the electrical angles between the coil sides, but they do not take into account the reinforcing action due to the tooth-slot alternations: considering that for  $h = 15, 30, 45, \dots$  the harmonic tooth fluxes have a number of North poles equal to the number of South poles within the coil pitch  $y_c = 5$ , it follows that the corresponding winding factors are zero;
- vice versa, the toothling factors consider the effect of the teeth: during the rotation, in sequence all the North poles of these harmonic fluxes with  $h = 15, 30, 45, \dots$  are at first faced to all the teeth and then to all the slots, producing an alternating flux linkage, with frequency  $f_h = h \cdot f_n$ ;

- nevertheless, these harmonic fluxes are homopolar fluxes and cannot return via the air-gap, but only between the front surfaces of the stator and rotor magnetic lamination stacks;
  - considering that the equivalent permeance (developing in air) crossed by these homopolar fluxes has a value of the order of the interpolar leakage permeance, the amplitude of these fluxes is always greatly lower than that of the heteropolar harmonic fluxes; moreover, if there is a skewing of one stator slot between slots and pole shoes, these homopolar harmonic fluxes are exactly zero.
- In conclusion, both on the basis of the classical theory and by considering the harmonic tooth fluxes, one can conclude that, for a symmetrical machine with the data of Table I, the harmonic fluxes with order  $h = 15, 30, 45, \dots$  are practically zero.

### COMPARATIVE ANALYSIS BETWEEN CALCULATION RESULTS AND EXPERIMENTAL TESTS

The application of the described method is illustrated with reference to the synchronous generator having the data of Table I. The machine has been equipped with one turn disposed around a stator tooth, in order to measure the e.m.f. induces in this turn during the no-load operation: the time integral of this e.m.f. gives the experimental waveform of the tooth flux.

The fig.2 shows the calculated and measured waveform of the tooth flux  $\varphi(t)$ , with frequency  $f = 50$  Hz and field current  $I_e = 1$  A; Table II shows the amplitudes of the corresponding harmonics, represented in a logarithmic form in the histograms of fig.3.

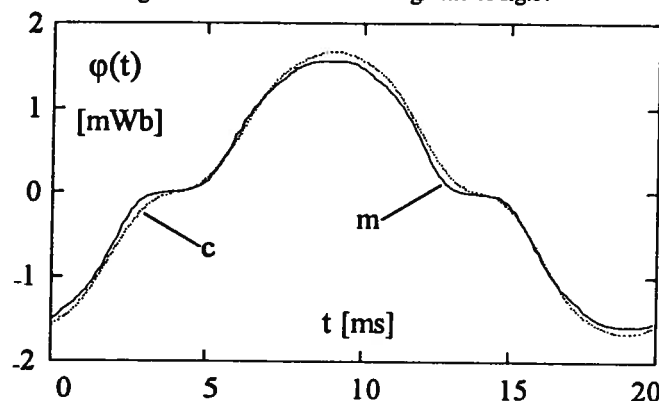


Fig.2 - Waveforms of the tooth flux of the synchronous machine of Table I;  $f = 50$  Hz;  $I_e = 1$  A; c = calculated; m = measured.

Table II - Harmonics of the tooth flux of the machine of Table I.

h	$\Phi_h$ meas. [ $\mu$ Wb]	$\Phi_h$ calc. [ $\mu$ Wb]	h	$\Phi_h$ meas. [ $\mu$ Wb]	$\Phi_h$ calc. [ $\mu$ Wb]
1	1440	1520	25	0.578	0.771
3	231	221	27	0.431	0.562
5	122.4	98.6	29	0.051	0.056
7	37.4	16.5	31	0.030	0.009
9	3.68	2.40	33	0.033	0.098
11	15.9	4.09	35	0.012	0.051
13	0.660	0.793	37	0.059	0.097
15	0.130	0.000	39	0.057	0.014
17	0.118	0.416	41	0.056	0.041
19	0.052	0.031	43	0.054	0.139
21	1.16	0.343	45	0.012	0.000
23	0.782	0.379	47	0.007	0.011

The following remarks can be made:

- the waveforms are quite close each other: it can be observed a different peak value; moreover, each half-wave of the measured tooth flux does not show specular symmetry as regards its axis:

this feature can be attributed to the hysteresis behaviour of the stator ferromagnetic core;

- both the calculated and the measured spectrum do not contain even harmonics having significant amplitude; this comes into line with what theoretically predictable: as a matter of fact, on the one hand, the hysteresis does not generate even harmonics; on the other hand, the absence of even harmonics means that the rotor structure does not have dissymmetries (all the poles have the same constructional characteristics, presumably because they have been obtained by means of subsequent punchings with the same tool);
- by observing the histograms of fig.3, we can state that the general aspect of the calculated spectrum is quite close to that of the measured one, except for some significant differences (in particular for the harmonics with order 15 and 45);
- by applying eq.(24) to the calculated and measured values of the tooth fluxes and with the values of  $\sigma_h$  for  $y_c = 5$  we obtain the following values respectively:  $THD_c = 1.66\%$ ;  $THD_m = 2.28\%$ .

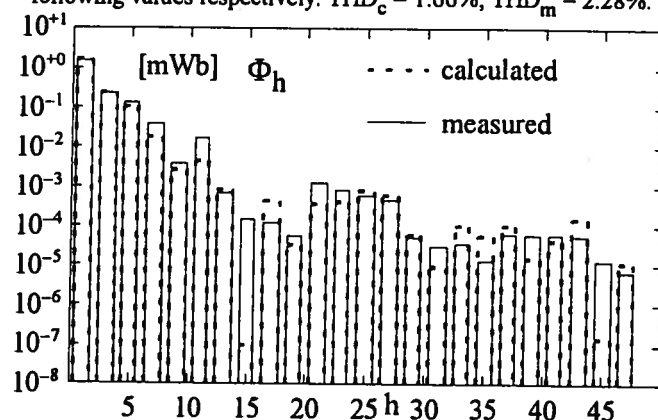


Fig.3 - Amplitudes of the tooth flux harmonics corresponding to the waveforms of fig.2 and to the values of Table II;  $f = 50$  Hz;  $I_e = 1$  A; just the odd measured harmonics are shown, because they are prevailing compared with the even ones.

The differences between calculated and measured quantities can be attributed to different concurrent causes, whose comparative importance is difficult to be estimated separately:

- of course, one part of the differences can be attributed to the model inaccuracies, in particular as regards the tooth reluctances at the air-gap: concerning this, the choice of a low value of the field current leads to make prevailing the effect of the magnetic voltage drop at the air-gap, both for the calculated values and for the experimental ones: in this way it is possible, at least partially, to reduce the uncertainties of the knowledge of the lamination B(H) curve, that is involved in the evaluation of the magnetic voltage drops in the ferromagnetic branches; in conclusion, doing this, the portion of the differences due to the inaccuracies of the calculation method depends mainly on the errors in the model of the tooth reluctances at the air-gap, that represent the parameters of the magnetic network more difficult to be evaluated;
- one part of the differences can be attributed to the constructional inaccuracies due to manufacture and assembling: the tested machine, taken from the standard production, is characterised by stator internal and rotor external diameters whose value is assured with tolerances of  $\pm 50$   $\mu$ m: considering that these tolerances can be partially interpreted in terms of stator and/or rotor eccentricities, significant variations of the actual value of the minimum air-gap width at the centre of the pole (seen by each stator tooth along the machine periphery) can occur, compared with the nominal value (up to  $\pm 8$  % roughly); this eccentricity, in addition to a different value of this minimum air-gap, implies also a modulation of the air-gap seen by each tooth during the rotation; thus, each tooth can be interested by a tooth flux with different peak value and waveform, with significant discrepancies in the har-



monic spectrum of the tooth fluxes from one tooth to the others, and compared with the tooth flux of the nominal symmetrical case considered for the model calculations;

- finally, one portion of the differences must be attributed to the measurement errors, also considering that, due to the low amplitude of some harmonics in the spectrum, the dynamics of the signal to be analysed is of the order of the spectral resolution of the FFT spectrum analyser (12 bits): concerning this problem, with the aim to improve the spectral resolution, a measurement technique based on the cancellation of the fundamental component (separately measured) has been adopted, in such a way to measure as better as possible the amplitudes of just the harmonics.

As a confirmation of the previous remarks, in the following the calculated and measured spectra of the phase e.m.f. odd (prevailing) harmonics of the machine of Table I are analysed, expressed in p.u., again for  $I_e = 1$  A: fig.4 shows these spectra in terms of histograms in logarithmic scale, in order to allow a global examination (the represented measured harmonics are those of the phase A only), while Table III contains all the values (the measured values are those of the three phases: A, B, C).

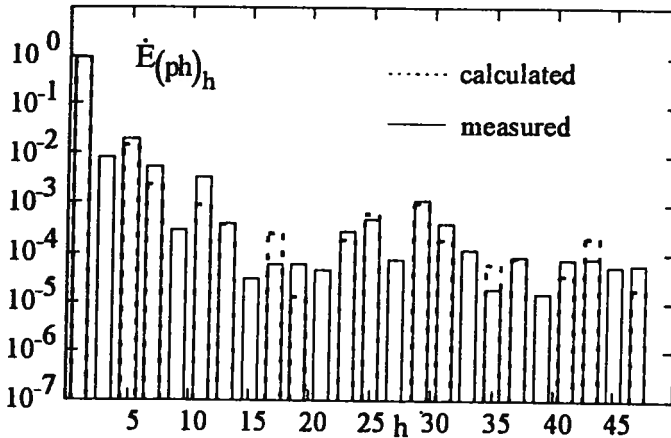


Fig.4 - Spectrum of the p.u. amplitudes of the calculated and measured phase e.m.f.s (phase A) of the machine of Table I;  $f = 50$  Hz;  $I_e = 1$  A; all the harmonics are referred to the fundamental phase e.m.f. calculated value ( $E_{ph1(calc.)} = 161.4$  V<sub>RMS</sub>); the corresponding THD<sub>ph</sub> values are: THD<sub>(calc.)</sub> = 1.66 % ; THD<sub>(meas.)</sub> = 2.49 %.

Table III - Amplitude spectrum of the calculated and measured phase e.m.f.s, corresponding to the conditions of the histograms of fig.4:  $f = 50$  Hz;  $I_e = 1$  A; all the harmonics are referred to the fundamental phase e.m.f. calculated value ( $E_{ph1(calc.)} = 161.4$  V<sub>RMS</sub>); in the table the following symbol have been used:  $10^{-3} = m$ .

h	$\dot{E}(ph)_h$ calculated	$\dot{E}(phA)_h$ measured	$\dot{E}(phB)_h$ measured	$\dot{E}(phC)_h$ measured
1	1	0.965	0.971	0.961
3	0	8.66 m	7.71 m	10.11 m
5	16.29 m	21.24 m	20.24 m	19.46 m
7	2.48 m	5.74 m	5.90 m	5.32 m
9	0	0.294 m	0.191 m	0.169 m
11	0.947 m	3.52 m	3.45 m	3.63 m
13	0.371 m	0.397 m	0.059 m	0.360 m
15	0	0.029 m	0.116 m	0.091 m
17	0.255 m	0.059 m	0.103 m	0.092 m
19	0.012 m	0.061 m	0.088 m	0.030 m
21	0	0.044 m	0.015 m	0.017 m
23	0.186 m	0.287 m	0.346 m	0.320 m
25	0.637 m	0.493 m	0.456 m	0.552 m
27	0	0.074 m	0.111 m	0.107 m
29	1.07 m	1.21 m	1.31 m	1.08 m

The following remarks can be made:

- the calculated values of Table III have been obtained as output of the program that calculates the e.m.f. harmonics by means of the eq.s (13), starting from the flux linkages evaluated by the eq (6), once known all the teeth fluxes for each position  $\gamma(t)$ : we have verified that these results are exactly the same obtained by the phasor sum using the toothing factors, expressed by eq.(24);
  - the existence of a significant constructional dissymmetry of the machine is evident just considering the phase fundamental e.m.f. values, different each others and lower of 3-3.5 % compared with the calculated value: this can be justified with the existence of eccentricities and of air-gap diameters different from the rated one;
  - the eccentricity is clearly confirmed by the presence of significant amplitudes of the phase harmonics of order 3 and multiples ( $h = 9, 15, 21, 27, \dots$ ), that with  $\gamma_c = 5$  should be zero;
  - the difference between harmonics of equal order measured in the three phases (for example, for  $h = 9, 13, 17, 21$ ) can be partially due to the constructional dissymmetries, and partially attributed to the measurement inaccuracies during the spectral analysis;
  - the percent differences between the calculated and measured harmonic amplitudes (for example,  $h = 5, 7, 11, 13, 23, 25$ ) is close to that between the corresponding values of the tooth flux harmonics of Table II; these differences are generally much lower compared with the measured amplitudes of the harmonics 3 and multiples (that should be exactly zero in case of a symmetrical machine);
  - it is interesting to observe that the first tooth harmonic actually present in the spectrum ( $h = 29$ ) shows a calculated value quite close to those measured in the three phases, with a difference roughly of the same value and sign of that between the corresponding tooth flux harmonics of Table II;
  - it can be noted that these phase e.m.f. harmonics for  $h = 29$  have a higher amplitude compared with the amplitude of the harmonics with near order: for example, the e.m.f. harmonic with order  $h = 25$  is roughly 2.5 times lower than the harmonic with order 29, even if the tooth harmonic flux with  $h = 29$  approximately equals one tenth the tooth harmonic flux for  $h = 25$ . This is due to the fact that with  $\gamma_c = 5$  the toothing factor for  $h = 29$  is the same of the fundamental one, while the toothing factor for  $h = 25$  is much lower (see fig.1:  $\sigma_{25}/\sigma_{29} \approx 0.05$ ).
- For a further, decisive confirmation of the existence of a significant eccentricity between stator and rotor, some spectral measurements even on the line-to-line e.m.f.s have been performed: also these voltages have shown the presence of harmonics of order 3 and multiples; in particular, for the 3<sup>rd</sup> harmonic, assumed the same reference of Table III, here used in terms of line-to-line quantity ( $V_{ref} = \sqrt{3} \cdot E_{ph1(calc.)} = \sqrt{3} \cdot 161.4$  V<sub>RMS</sub>, again for  $I_e = 1$  A), we obtained:
- $\dot{E}_{AB(3)} = 0.0078$  p.u.;  $\dot{E}_{BC(3)} = 0.0091$  p.u.;  $\dot{E}_{CA(3)} = 0.0098$  p.u..

## DESIGN REMARKS

In the following, some design analysis results are shown, with the aim to show the dependence of the waveforms and of the harmonic distortion on some machine constructional and operating quantities.

It is interesting to examine the effect of the saturation of the ferromagnetic circuit on the calculated and measured waveforms of the ratio  $\phi(t)/I_e$ , between the tooth flux and the field current generating that flux, for field currents of 1 A and 2 A: if the magnetic voltage drop remained negligible, the curves of the tooth flux/field current should not change when increasing  $I_e$ ; vice versa, the lowering and the flattening of the curve  $\phi(t)/I_e$  for  $I_e = 2$  A testifies a significant effect of the saturation, with distinct deformation and alteration of the waveform harmonic content. Considering that, as shown, the harmonic spectrum of the tooth flux affects the harmonic distortion of the waveforms at the terminals, it follows a distortion increase.

The comparison between the waveforms of fig.5 suggests that there is a discrete correspondence among calculations and measurements; nevertheless, the correct evaluation of the harmonics when the satu-



ration increases becomes more difficult, both for the uncertainties in the knowledge of the B(H) curve, and because of the amplification that the increase of the saturation has on the distorting effect of the constructional dissymmetries.

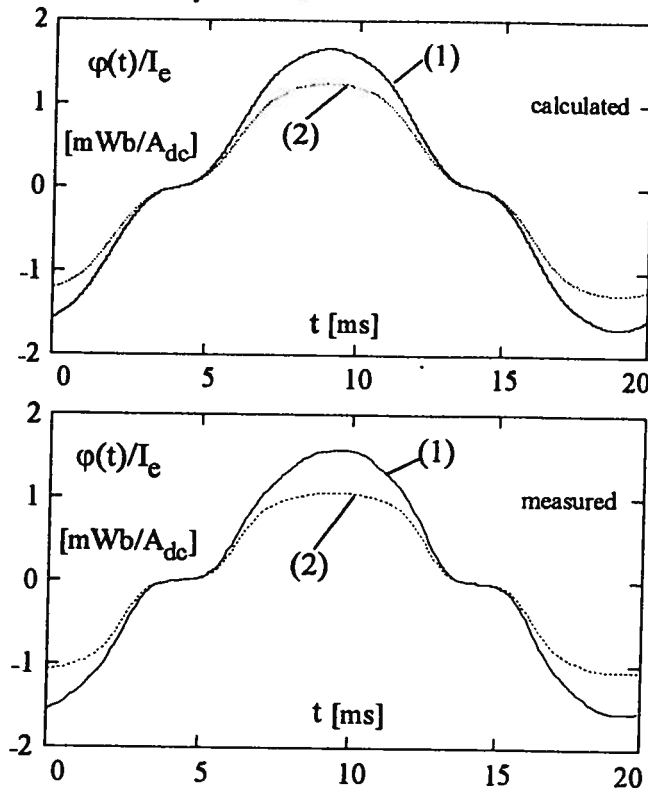


Fig.5 - Effect of the saturation on the waveform of the tooth flux  $\phi(t)$ : curves of the ratio  $\phi(t)/I_e$ , for the two following cases:

(1):  $I_e = 1 A_{dc}$ ; (2):  $I_e = 2 A_{dc}$ ;  
above: calculated curves; below: measured curves.

Fig.6 shows the dependence of the calculated waveform of the tooth flux  $\phi(t)$  on the increase of the internal stator diameter, increase equal to the mechanical tolerance declared by the manufacturer ( $\Delta D_M = 50 \mu m$ ), considering a perfect centring between stator and rotor: it can be observed that the difference among the two  $\phi(t)$  curves is of the same order of that between the calculated and the experimental curves of fig.2, that have led to the tooth flux harmonics of Table II, whose differences have been already discussed.

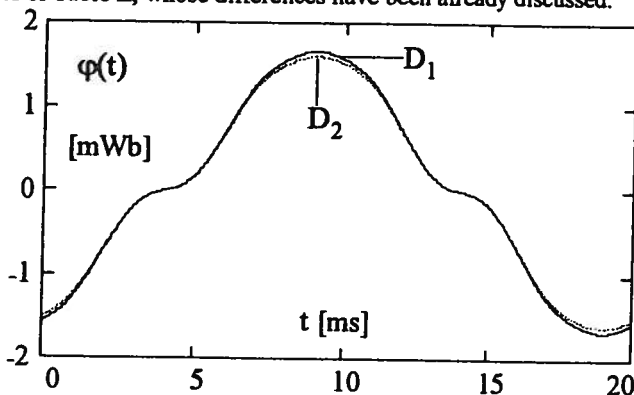


Fig.6 - Calculated waveform of the tooth flux  $\phi(t)$ , with field current  $I_e = 1 A$ : effect of a growth of the stator internal diameter, equal to the maximum mechanical tolerance:

$D_1 = D = 160 \text{ mm}$ ;  $D_2 = D + \Delta D_M = 160.05 \text{ mm}$ .

Actually, if we consider also the inevitable eccentricity between stator and rotor, the waveforms of  $\phi(t)$  can be even more different

one from the other compared with the discrepancy of fig.5, and, as a consequence, also their tooth flux harmonics can be modified.

Finally, Table IV shows how the amplitude of the fundamental and of the harmonic phase e.m.f.s is affected by a shortening of the coil pitch, starting from the full pitch ( $y_c = 7 \approx s/p$ ), through the classical shortening ( $y_c = 6 \approx (5/6)s/p$ ), up to the shortening value adopted in the tested machine ( $y_c = 5$ ), the calculations have been again developed for  $I_e = 1 A$ .

Table IV - Calculated amplitude of the fundamental and harmonic phase e.m.f.s as a function of the coil pitch  $y_c$ , with  $I_e = 1 A$ , for the machine of Table I.

h	$E_h [V_{RMS}]$ ( $y_c = 7$ )	$E_h [V_{RMS}]$ ( $y_c = 6$ )	$E_h [V_{RMS}]$ ( $y_c = 5$ )
1	185.345	177.245	161.398
3	18.506	11.438	0
5	2.629	0	2.629
7	0.344	0.272	0.400
9	0.088	0.142	0
11	0.072	0.168	0.153
13	0.014	0.041	0.06
15	0	0	0
17	0.01	0.028	0.041
19	0.001	0.002	0.002
21	0.029	0.047	0
23	0.026	0.020	0.030
25	0.103	0	0.103
27	0.424	0.262	0
29	0.197	0.189	0.172

The following remarks can be made:

- the successive pitch shortening reduces the amplitude of the fundamental e.m.f. (for the effect of the simultaneous reduction of the tooth factor);
- in return, the 3<sup>rd</sup> harmonic, which has the most important amplitude, is significantly reduced, till to become zero for  $y_c = 5$ ;
- the 5<sup>th</sup> harmonic becomes zero when changing from  $y_c = 7$  to  $y_c = 6$ , and then it comes back to the original value;
- the higher order harmonics are subjected to alternated events, but in general we can say that, because of their amplitude reduction when considering increasing order, they give a smaller contribution to the THD (except for the orders 27 and 29, that present again significant amplitudes, being close to the tooth harmonic orders).

On the basis of these remarks, it could seem suited and obliged the adoption of a coil pitch equal  $y_c = 5$ , as actually chosen by the manufacturer, in fact, in terms of line-to-neutral voltage, for the three considered pitches the following values of the phase voltage THD have been obtained (for  $I_e = 1 A$ ):

$y_c$	7	6	5
THD <sub>ph</sub> [%]	10.09	6.46	1.66

These values confirm the soundness of the choice  $y_c = 5$ .

On the other hand, if we consider the line-to-line voltages, the cancellation of the harmonics with order 3 and multiples (of course, in case perfectly symmetrical machine) implies that the most favourable solution is that with  $y_c = 6$ , as shown by the line-to-line voltage THD value (THD<sub>l</sub>):

$y_c$	7	6	5
THD <sub>l</sub> [%]	1.44	0.24	1.66

It can be observed how the THD in the case  $y_c = 5$  is the same for the line-to-neutral and for the line-to-line voltages, as a consequence of the fact that with this pitch the harmonics with order 3 and multiples are already zero in the line-to-neutral e.m.f.

On the other hand, it must be recognised that among the factors of merit examined by the manufacturer in order to choose the winding pitch  $y_c$ , besides the waveform distortion aspects, there are also estimations concerning some other constructional and operating elements: as a matter of fact, thanks to the lower length of the end-windings connected with the adoption of an adequately shortened pitch, it is possible to achieve a saving both in the copper amount used for the windings and a reduction of the winding Joule losses.

### **CONCLUSIONS**

The present paper has described and applied a method for the determination of the harmonic distortion of the no-load voltage of salient-pole alternators: by means of this method it is possible to consider the winding features, the shape of the pole shoes, the presence of the slots, the rotor-stator skewing, the saturation of the ferromagnetic branches and the conditions of eccentricity and other constructional dissymmetries.

In the case of a perfectly symmetrical machine it has been shown how the time waveform of the tooth flux acts in generating the phase flux linkage and then the waveform and the harmonics of the line-to-neutral and of the line-to-line e.m.f.s: noticeable analytical relations that give the expression of the THD have been obtained, that link the distortion level to some winding-dependent coefficients (that operate, for each harmonic, the phasor sum of the teeth-coil linkage coefficients) and to the time harmonics of the tooth fluxes.

The comparison between calculated and experimental values for a salient-pole standard machine have given good results as regards the substantial soundness of the calculation method, also considering the remarkable uncertainties concerning the exact dimensions of the magnetic core of the machine (manufacture tolerances) and as regards the measurement errors of the FFT spectral analysis.

Some calculation examples have shown the influence of the operating conditions (saturation), of the size changing (stator internal diameter) and of the choice of the coil pitch.

The activity on this subject will continue, according to the following research lines:

- improvement of the model, in particular as regards the more accurate calculation of the tooth permeances at the air-gap;
- development and completion of the experimental tests, also with other machines, if possible characterised by accurate manufacture tolerances;
- theoretical analysis about the impact of the constructional defects on the levels of voltage distortion and voltage dissymmetry;
- extension of the method to the analysis of the voltage distortion in loaded operation.

### **REFERENCES**

- [1] Di Gerlando, R. Perini, I. Vistoli: "Evaluation of No-Load Voltage Harmonics of Salient-Pole A.C. Generators: Analytical-Numerical Methodologies"; Proceedings of VI ICHPS, Bologna, Italy, 1994, pp.104-110.
- [2] A. Di Gerlando, R. Perini, I. Vistoli: "Analytical Modelling of the Field at the Air-gap of Salient-pole A.C. Generators for the Estimation of the No-load Voltage Harmonics"; Proceedings of VI ICHPS, Bologna, Italy, 1994, pp.97-103.
- [3] A. Di Gerlando, R. Perini, I. Vistoli: "A Field-Circuit Approach to the Design Oriented Evaluation of the No-Load Voltage Harmonics of Salient-Pole Synchronous Generators"; Electrical Machines and Drives Conference Proceedings, Durham, United Kingdom, 1995, pp.390-394.